Published in final edited form as:
J Immunol. 2007 November 15; 179(10): 6561–6567.

Intrahepatic Lymphocyte Expression of Dipeptidyl Peptidase I-Processed Granzyme B and Perforin Induces Hepatocyte Expression of Serine Proteinase Inhibitor 6 (*Serpinb9*/SPI-6)[1]

Heather W. Stout-Delgado[*,†], **Yonas Getachew**[*], **Bonnie C. Miller**[*,†], and **Dwain L. Thiele**[2,*,†]

[*]*Department of Internal Medicine, Division of Digestive and Liver Diseases, University of Texas Southwestern Medical Center, Dallas TX 75390*

[†]*Immunology Graduate Program, University of Texas Southwestern Medical Center, Dallas TX 75390*

Abstract

Human proteinase inhibitor 9 (PI-9/*serpinB9*) and the murine ortholog, serine proteinase inhibitor 6 (SPI-6/*serpinb9*) are members of a family of intracellular serine proteinase inhibitors (serpins). PI-9 and SPI-6 expression in immune-privileged cells, APCs, and CTLs protects these cells against the actions of granzyme B, and when expressed in tumor cells or virally infected hepatocytes, confers resistance to killing by CTL and NK cells. The present studies were designed to assess the existence of any correlation between granzyme B activity in intrahepatic lymphocytes and induction of hepatic SPI-6 expression. To this end, SPI-6, PI-9, and *serpinB9* homolog expression was examined in response to IFN-α treatment and during in vivo adenoviral infection of the liver. SPI-6 mRNA expression increased 10- to 100-fold in the liver after IFN-α stimulation and during the course of viral infection, whereas no significant up-regulation of SPI-8 and <5-fold increases in other PI-9/*serpinB9* homolog mRNAs was observed. Increased SPI-6 gene expression during viral infection correlated with influxes of NK cells and CTL. Moreover, IFN-α-induced up-regulation of hepatocyte SPI-6 mRNA expression was not observed in NK cell-depleted mice. Additional experiments using genetically altered mice either deficient in perforin or unable to process or express granzyme B indicated that SPI-6 is selectively up-regulated in hepatocytes in response to infiltration of the liver by NK cells that express perforin and enzymatically active granzyme B.

Increased numbers of activated NK cells and CTL infiltrate the liver during systemic (1) and localized immune responses (2). These cytotoxic effector cells play an essential role in the clearance of noncytopathic viruses from infected tissues (3–5). NK and NKT cells also amplify hepatocellular injury initiated by non-infectious causes of liver injury (6). Virally infected hepatocytes are resistant to killing by the perforin and granzyme-dependent cytotoxic effector pathway (7), the predominant killing pathway utilized by CTL and NK cells in clearance of noncytopathic viruses from many nonhepatic tissues. Consequently, Fas ligand and TNFR-mediated killing mechanisms play a more prominent role in clearance of viral infection from the liver than is observed during clearance of viral infections from extrahepatic sites (7–9).

[1]This research was supported by National Institutes of Health Grant 5RO1 DK53933.

[2]Address correspondence and reprint requests to Dr. Dwain L. Thiele, Department of Internal Medicine, 5323 Harry Hines Boulevard, Dallas, TX 75390-9030. E-mail address: dwain.thiele@utsouthwestern.edu

The costs of publication of this article were defrayed in part by the payment of page charges. This article must therefore be hereby marked *advertisement* in accordance with 18 U.S.C. Section 1734 solely to indicate this fact.

Disclosures: The authors have no financial conflict of interest.

Granzyme B, a serine proteinase present in the specialized cytotoxic granules of NK cells and CTL, plays a key role in the induction of cell death mediated by granule exocytosis effector mechanisms (4). Granzyme B is synthesized as an inactive zymogen and requires the removal of its propeptide by cathepsin C/dipeptidyl peptidase I (DPPI)[3] for activation (10). Human proteinase inhibitor 9 (PI-9) and the murine ortholog serine proteinase inhibitor (SPI) 6 are members of a family of OVA serpin inhibitors present in immune-privileged cells, APCs, and CTLs that afford protection against the actions of granzyme B (11–13). When expressed in tumor cell lines or embryonic stem cells, PI-9 (14–17) and SPI-6 (18–20) confer resistance to perforin/granzyme B-mediated killing by CTL and NK cells. Recent studies have indicated that induction of SPI-6 expression in hepatocytes during hepatic viral infection (21) modulates sensitivity to cytotoxic lymphocyte effector mechanisms and the severity of liver injury during viral infection of the liver (22).

In contrast to the human genome, which appears to contain only a single *serpinB9* gene, the mouse genome contains multiple *serpinB9* homologs identified by sequence similarities (18). The target or cognate proteases associated with these additional *serpinB9* homologs are not yet known. In contrast to stable patterns of SPI-6 expression in the spleen and various immune privileged sites, in liver, induction of SPI-6 expression from very low background levels has been observed only following viral infection (21) or following administration of IFN-α (22). The current studies were designed to further characterize the pattern of serpin expression in the liver during viral expression and initiate investigation of mechanisms responsible for hepatocyte expression of SPI-6 in vivo.

Materials and Methods

Mice

C57BL/6J (B6) and perforin knockout (B6.*pfp*) mice were obtained from The Jackson Laboratory. Granzyme B knockout mice backcrossed on the B6 background for >20 generations (B6.*gzmb*$^{-/-}$) were generously provided by Dr. T. Ley (Washington University, St. Louis, MO) (23). DPPI (B6.*dpp1*$^{-/-}$) mice were generously provided by Dr. C. Pham (Washington University) (10). Mice used in individual experiments were age and sex matched and used before 12 wk of age. No gender differences in levels or regulation of SPI-6 expression were noted in these experiments. All animal studies were conducted in compliance with accepted standards of humane animal care and were approved by the University of Texas Southwestern Institutional Animal Care and Use Committee.

Adenovirus vector

An E1-deleted, replication deficient, β-galactosidase encoding recombinant adenovirus AdCMV-*lacZ* was propagated in 293 cultures, purified on a cesium chloride gradient, and virus

[3]Abbreviations used in this paper

DPPI dipeptidyl peptidase

PI-9 proteinase inhibitor 9

OPU optical particle unit

SPI-6 serine proteinase inhibitor 6

BLT *N*-α-benzyloxy-carbonyl-L-lysine thiobenzyl

titers were quantified by A260:280 ratio as previously described (8,24). Mice were injected via the tail vein with 10^{10}–to 10^{11} optical particle units (OPU) of AdCMV-*lacZ* to produce hepatic adenoviral infection as previously described (7).

β-Galactosidase assay

β-Galactosidase activity was quantified by measuring the rate of cleavage of 4-methylumbelliferyl-*β*-D-galactoside to yield the fluorescent product 4-methylumbelliferone, as previously described (7,8).

Real-time PCR

Real-time RT-PCR primer sets were designed using PRIMER EXPRESS software (Applied Biosystems). Real-time PCR were performed in a final volume of 10 *μ*l containing cDNA from 20 ng of reverse-transcribed total RNA, 150 nM forward and reverse primers, and SYBR Green Universal PCR Master Mix (Applied Biosystems). PCR was conducted in 384 well plates using the Applied Biosystems Prism 7900HT Sequence Detection System (Applied Biosystems). All reactions were performed in triplicate. Melting curve analyses and serial dilution were performed to identify primer sets and conditions yielding specific products quantitatively over a wide range of input cDNA. Primers validated by this technique and used in the present studies were *serpinb9*, *serpinb9b*, *serpinb9c*, *serpinb9e*, *serpinb9f*, *serpinb9g*, cyclophilin, 18S RNA, KLRK1, and CD3*ε* (Table I). Relative levels of mRNA were calculated by the comparative cycle threshold method (User Bulletin No. 2; Applied Biosystems). Cyclophilin mRNA and/or 18S RNA levels were used as the invariant control for all studies.

Western blotting

Cells were washed, suspended in lysis buffer (20 mM HEPES (pH 7.2), 10 mM KCl, 5 mM $MgCl_2$,1 mM EDTA, 250 mM sucrose, and proteinase inhibitors (Sigma-Aldrich)), lysed by repeated freeze-thawing, and centrifuged for 10 min at 10,000 × *g* to remove debris, as previously described (21). Protein concentrations in tissue homogenates were assayed by the bicinchoninic acid method with reagents purchased from Pierce and using BSA as a standard. Equal amounts of total cytosolic protein (20 or 40 *μ*g/lane) were separated on 15% bis-acrylamide gels by SDS-PAGE and electrophoretically transferred to nitrocellulose in pH 9.9 carbonate buffer. Immunodetection was performed using primary anti-SPI-6 and secondary HRP-conjugated anti-rabbit Ig and the ECL Western Blotting Analysis System (Amersham Pharmacia Biotech).

IFN-α administration

Recombinant human IFN-*α*2b (INTRON A) was obtained from Schering-Plough. Mice were injected i.p. IFN-*α* and selected tissues were harvested 24–48 h after treatment as previously described (9). Previous work has indicated that in vivo administration of human IFN-*α* A/D (25) or IFN-*α*2b (26) in mice leads to hepatic accumulation of NK cells while in vitro exposure to murine IFN-*α* leads to induction of SPI-6 expression in hepatocytes (21).

NK cell depletion

Mice were treated with 15 *μ*g of anti-asialo GM1 Ab (WAKO) starting 2 days before human rIFN-*α* (IFN-*α*2b/INTRON; Schering-Plough) administration. The control mice received equal amounts of rabbit IgG isotype control Ab (Sigma-Aldrich). In preliminary studies, this anti-asialo GM1 treatment regimen was found to deplete >95% of $NK1.1^+CD3^-$ NK cells, but only ~20% of $NK1.1^+CD3^+$ NK T cells from the liver of IFN-*α*-treated mice.

Isolation of intrahepatic lymphocytes and hepatocytes

The abdomen of anesthetized mice was entered using a sterile technique, the portal vein was cut, and the abdominal portion of the vena cava was perfused with 10-ml of Ca^{2+}- and Mg^{2+}-free phosphate buffer solution preheated to 37°C. The liver was removed and passed through a 40-mesh pore size screen, then a 300-mesh pore size screen (VWR Scientific) (27). The cell suspension was centrifuged at 400 × *g* for 15 min and the cell pellet was resuspended in 40% Percoll and underlayered with an equal volume of 70% Percoll. The gradient was centrifuged at 900 × *g* for 20 min and lymphocytes were isolated from the 40–70% interface. Cells were washed with RPMI 1640 medium (Invitrogen Life Technologies). Primary murine hepatocytes were isolated as previously described (7,28).

DPPI and N-α-benzyloxy-carbonyl-$_L$-lysine thiobenzyl (BLT) esterase assays

DPPI activity was assayed by the hydrolysis of glycylphenylalanyl-*β*-napthylamide (100 μM) as previously described (7,29,30). Substrate hydrolysis was monitored by the fluorescence of *β*-naphthylamine released per minute per milligram of protein. BLT esterase activity was assayed as previously described (7). The mixture was incubated at 37°C and the change in absorbance at 410 nm was measured and compared with that in samples containing no cell extract.

Bone marrow transplantation

On the day of transplantation, the age- and sex-matched B6, B6.*dpp1*$^{-/-}$, and B6.*gzmb*$^{-/-}$ recipients were irradiated (800 cGy) and 2 h later were injected via the lateral tail vein with donor cells. A total of 8×10^6 bone marrow cells from B6, B6.*dppi*1$^{-/-}$, or B6.*gzmb*$^{-/-}$ mice was injected into the lateral tail vein of these lethally irradiated syngeneic B6, B6.*dpp1*$^{-/-}$, or B6.*gzmb*$^{-/-}$ mice as previously described (31). Recipients were maintained on acidified (pH 2) antibiotic (100 mg/L neomycin and 10 mg/L polymyxin B) H_2O for 7 days after transplantation.

Results

Serpinb9 (SPI-6) is the only homolog of serpinB9 (PI-9) that is up-regulated >10-fold during hepatic viral infection

SerpinB9 (PI-9) and the murine homolog *serpinb9* (SPI-6) were found in previous studies to be up-regulated in hepatocytes in vitro by the antiviral cytokine IFN-*α* (21). To investigate the in vivo effect of IFN-*α* on hepatic expression of SPI-6 and other *serpinB9* homologs, B6 mice were treated with varying doses of human rIFN-*α*. At 24 h after administration, liver tissue was harvested and murine *serpinB9* homolog mRNA levels were analyzed using real-time PCR. As illustrated in Fig. 1, *top panel*, SPI-6 mRNA expression was increased ~7-fold above background in recipients of 0.4 U/g IFN-*α* with higher levels of SPI-6 mRNA induction (30- to 40-fold) observed after administration of larger IFN-*α* doses. Of note, up-regulation of SPI-6 mRNA was observed following i.p. administration of lower doses of IFN-*α* than required for induction of hepatic mRNA levels of the well characterized IFN response gene PKR. Following administration of lower doses of IFN-*α*, SPI-6 was the only *serpinB9* homolog gene significantly up-regulated. Although modest induction of *serpinb9b*, *serpin9c*, and *serpin9f* mRNA expression was observed after administration of very high doses of IFN-*α*, expression of these serpin genes was not increased to levels comparable to those of SPI-6. mRNA levels of two additional *serpinB9* homologs, *serpin9g* and *serpin9e*, remained unaltered even in recipients of very high doses of IFN-*α* (data not shown). mRNA expression of constitutively expressed genes, such as cyclophilin and SPI-8, a serpin previously observed to be expressed in normal liver (21,32), also remained unaltered over a broad range of IFN-*α* dosing.

To assess *serpinB9* homolog expression during viral infection, B6 mice were infected with 4×10^{10} OPU of AdCMV-*LacZ* via a single tail vein injection. As illustrated in Fig. 1, *bottom panel*, a nearly 10-fold increase in SPI-6 mRNA expression was detected at day 1, with further increases over time. Peak gene expression, nearly 100-fold baseline, was detected at day 8. In contrast, *serpinb9b*, *serpin9c*, and *serpin9f* mRNA levels in the liver were not increased >3-fold at any point during adenoviral infection while *serpin9g* and *serpin9e* mRNA levels remained unaltered during the course of viral infection (data not shown).

Expression and processing of granzyme B modulates SPI-6 expression

To assess whether SPI-6 expression correlates with an increase in hepatic lymphocyte granzyme B expression following IFN-*α* administration, a therapy previous noted to induce hepatic infiltration of NK cells (26), IFN-*α* was administered to wild-type and genetically modified B6 mice with selected defects in the perforin and granzyme B CTL effector pathway. In wild-type B6 (Fig. 2*A*) and B6.*dpp1*$^{-/-}$ mice (Fig. 2*B*), granzyme B mRNA increased and reached peak expression at 8 h after IFN-*α* administration. As illustrated in Fig. 2*A*, SPI-6 mRNA levels in livers from B6 mice increased after granzyme B mRNA levels had peaked and were increased 140-fold at 16 h after IFN-*α* administration. However, a <5-fold increase in SPI-6 expression was detected in livers of B6.*dpp1*$^{-/-}$ mice at 16 or 24 h after IFN-*α* administration (Fig. 2*B*). Since B6.*dpp1*$^{-/-}$ mice lack the DPPI activity required for posttranslational processing of granzyme B to an enzymatically active, mature enzyme, these results suggested a role for active granzyme B in the induction of SPI-6 expression in IFN-*α*-treated mice.

To determine whether SPI-6 expression was indeed dependent on normal expression and function of granzyme B, IFN-*α* was administered to other strains of mice with different defects in perforin/granzyme B-mediated cytotoxicity. In addition to B6.*dpp1*$^{-/-}$ mice that are defective in granzyme B processing, B6.*pfp*$^{-/-}$ mice that are defective in granzyme- and perforin-induced cytotoxicity, and B6.*gzmb*$^{-/-}$ mice that lack any granzyme B expression were examined for hepatic SPI-6 induction after IFN-*α* administration. As illustrated in Fig. 2*C*, a 40-fold increase in SPI-6 mRNA expression was observed in wild-type B6 mice at 24 h after IFN-*α* treatment while a <3-fold increase in SPI-6 mRNA expression in liver isolated from B6.*dpp1*$^{-/-}$, B6.*gzmb*$^{-/-}$, or B6.*pfp*$^{-/-}$ mice was observed.

To determine whether defects in perforin/granzyme B-mediated cytotoxicity also alters SPI-6 expression during viral infection, AdCMV-*LacZ* was administered via a single tail vein injection to B6, B6.*dpp1*$^{-/-}$, and B6.*gzmb*$^{-/-}$ mice. Mice were sacrificed at specific time points during viral infection and liver mRNA levels were analyzed by real-time PCR. SPI-6 mRNA expression was increased in B6 mice ~95-fold during viral infection and reached peak expression at day 8 (Fig. 2*D*). In contrast, SPI-6 mRNA expression increased <5-fold in AdCMV-*LacZ*-infected B6.*dpp1*$^{-/-}$ or B6.*gzmb*$^{-/-}$ mice (Fig. 2*D*).

To determine whether hepatic SPI-6 protein also was up-regulated during adenoviral infection in concert with changes in mRNA levels, AdCMV-*LacZ* was administered via a single tail vein injection to B6 and B6.*dpp1*$^{-/-}$ mice and SPI-6 expression in liver and spleen was assessed by immunoblotting. As illustrated in Fig. 3*A*, SPI-6 protein was not observed in uninfected livers of B6 or B6.*dpp1*$^{-/-}$ mice. However, constitutive expression was readily detected in spleens of both control (Fig. 3*A*) and AdCMV-*LacZ*-infected (data not shown) wild-type and B6.*dpp1*$^{-/-}$ mice. During viral infection, SPI-6 protein expression increased in the liver of B6 mice, becoming readily detectable at day 3 and remaining elevated for >20 days following viral infection (Fig. 3*B*). In contrast, no readily apparent SPI-6 protein expression was detectable by immunoblot analysis in livers of B6.*dpp1*$^{-/-}$ mice at days 3, 10, 15, or 25 after infection (Fig. 3*C*). Of note, similar *β*-galactosidase transgene expression levels were detected in the livers of each strain of mice in the experiments detailed in Figs. 2 and 3, confirming

equivalent levels of viral infection (data not shown). Moreover, similar levels of DPPI and BLT esterase activity (Fig. 4) in day 8 intrahepatic lymphocyte populations indicated equivalent levels of intrahepatic CTL/NK cell activation in B6.*gzmb*$^{-/-}$ and B6 mice during viral infection in these studies. Of note, the very low levels of BLT esterase activity in B6.*dpp1*$^{-/-}$ intrahepatic lymphocytes results from a lack of DPPI-mediated processing of pro-granzyme A to an enzymatically active form (29,30).

Up-regulation of SPI-6 mRNA correlates with increases in NK cell and CTL-specific gene expression in liver during viral infection

To determine whether increased SPI-6 expression correlated with increased infiltration of granzyme B- expressing NK cells and/or CTL, liver tissue was harvested from B6 mice at select time points during viral infection and levels of NK and CTL receptor mRNA expression were analyzed. As shown in Fig. 5, mRNA encoding KLRK1, an activation receptor present on the surface of NK cells, was increased ~65-fold by day 3. A >100-fold increase in mRNA levels of CD3ε at day 8 during viral infection was detected (Fig. 5).

These results suggest that initial up-regulation of SPI-6 expression in liver during AdCMV-LacZ infection immediately follows infiltration by NK cells and persists in parallel with the more prolonged presence of infiltrating T cells. To investigate whether the induction of hepatic SPI-6 expression following IFN-α treatment (Fig. 1) also correlates with the NK cell influx observed after i.p. IFN-α administration (26), mice were treated with an NK cell-depleting Ab, anti-asialo GM1, or an isotype control Ab 48 h before administration of IFN-α. In intrahepatic lymphocytes from control Ig-treated B6 mice, IFN-α administration resulted in an 8-fold increase in SPI-6 mRNA levels (Fig. 6). This increase in SPI-6 expression occurred in association with a 4- to 5-fold increase in the numbers of NK1.1^{+}CD3^{-} NK cells in livers of IFN-α-treated mice (data not shown). SPI-6 mRNA expression in hepatocytes isolated from control Ig-treated B6 mice was increased >50-fold at 24 h after IFN-α administration (Fig. 6*B*). In contrast, hepatocytes and intrahepatic lymphocytes isolated from NK cell-depleted mice did not show a significant increase in SPI-6 mRNA expression after IFN-α administration. These results suggest that the influx of granzyme B-expressing activated NK cells after IFN-α administration or during viral infection leads to an increase in cytoprotective SPI-6 expression by hepatocytes to protect against perforin/granzyme B-mediated killing.

Reconstitution of DPPI$^{-/-}$ mice with wild-type bone marrow results in SPI-6 expression after IFN-α stimulation

To determine whether the lack of SPI-6 expression in B6.*dpp1*$^{-/-}$ mice was due to the lack of enzymatically active granzyme B expression in intrahepatic lymphocytes or a defect in SPI-6 expression by DPPI-deficient hepatic parenchymal cells, B6.*dpp1*$^{-/-}$ mice were irradiated and reconstituted with bone marrow from wild-type mice and maintained for 6 wk to allow reconstitution of the immune system. DPPI assays of spleen samples confirmed DPPI expression in B6.*dpp1*$^{-/-}$ mice transplanted with wild-type bone marrow, indicating establishment of chimerism (data not shown). As shown in Fig. 7*A*, B6 or B6.*dpp1*$^{-/-}$ mice reconstituted with wild-type bone marrow exhibit SPI-6 protein expression in the liver after treatment with IFN-α. Similar results were obtained with B6.*gzmb*$^{-/-}$ mice reconstituted with wild-type bone marrow (data not shown). In contrast, wild-type B6 mice reconstituted with bone marrow derived from B6.*dpp1*$^{-/-}$ mice did not exhibit an increase in SPI-6 expression after IFN-α stimulation (Fig. 7*B*, *lanes 4* and *5*). These results indicate that the lack of hepatic SPI-6 expression in B6.*dpp1*$^{-/-}$ after IFN-α treatment or adenoviral infection is not related to any intrinsic defect in hepatic SPI-6 expression, but rather relates to lack of granzyme B activity in bone marrow-derived lymphocytes infiltrating the liver in response to these immune stimuli.

Discussion

These studies illustrate that increases in hepatocyte SPI-6 expression during viral infection correlate chronologically with the presence of activated, bone marrow-derived, granzyme B-expressing NK and CTL in the liver. Furthermore, mice lacking intact perforin or granzyme B do not exhibit similar levels of increased hepatic SPI-6 mRNA or protein expression after IFN-*α* administration or during AdCMV-LacZ infection. Thus, these findings indicate that the presence and likely release of DPPI-processed, enzymatically active granzyme B and perforin by bone marrow-derived cells that infiltrate the liver after IFN-*α* administration or during AdCMV-LacZ infection leads to the induction of SPI-6 expression in hepatocytes.

The mouse genome contains multiple *serpinB9* homologs (18,33). Putative mouse PI-9 homologs share >90% sequence homology with human PI-9. However, these homologs differ greatly from PI-9 in that they do not possess negatively charged residues in the P1 region of their reactive center loop (13,18,33,34). Other than sequence comparisons, the mouse homologs of PI-9 have not been well characterized previously. The current studies evaluated hepatic expression of SPI-6 and of additional PI-9 homologs, such as *serpinb9b/R86*, *serpin9c/NK9*, *serpin9d/NK21*, *serpin9e/NK21b*, and *serpin9g/NK26*, posttreatment with antiviral cytokines and during viral infection. The current findings indicate that SPI-6 is the only PI-9 homolog whose expression is up-regulated 10- to 100-fold in the liver after IFN-*α* administration or during the course of AdCMV-*LacZ* infection. Furthermore, the results of the present studies illustrate that SPI-6 expression correlates with granzyme B expression in that up-regulation in SPI-6 expression directly follows infiltration of the liver by granzyme B-expressing cytotoxic lymphocytes, but not by cytotoxic lymphocytes deficient in granzyme B expression, granzyme B processing, or perforin, an effector molecule that facilitates granzyme B entry into target cell cytosol.

Previous work has illustrated that the liver does not constitutively express PI-9 or SPI-6, which may indicate that these genes are tightly regulated and bound to a transcriptional repressor during normal conditions (13,18). The need for both enzymatically active granzyme B and perforin expression by intrahepatic lymphocytes during induction of high levels of SPI-6 expression in virally infected hepatocytes suggests a unique mechanism of SPI-6 gene regulation not previously noted in other cell lineages expressing SPI-6. Once inside the cytosol, granzyme B cleaves substrates that can induce apoptosis. Up-regulation of SPI-6 may occur as a direct result of granzyme B entry into hepatocytes or may be due to enzymatic cleavage and/or up-regulation of additional factors present in the cytosol that bind and induce SPI-6 gene transcription. Similar proteinase-mediated regulation of hepatocyte gene transcription has been noted to be mediated by caspase 3 (35), a known substrate of granzyme B (4). However, it is of interest that in the present studies, up-regulation of the granzyme B inhibitor SPI-6 occurred both during adenoviral infection, when caspase-dependent NK and CTL killing of virally infected hepatocytes is anticipated, and after IFN-*α* was administered in doses known to induce hepatic infiltration of highly activated NK cells but not known to induce perforin and granzyme B-mediated hepatocellular injury (25). It remains to be determined whether granzyme B- and perforin-dependent, IFN-*α*-induced SPI-6 expression also is related to mild levels of caspase-dependent hepatocellular injury induced by IFN-*α*-activated NK cells.

Previous studies from our laboratory indicate that an important role of *serpinb9*/SPI-6 expression in hepatocytes is to protect these cells from killing by granzyme B-expressing NK cells and CTL (22). Moreover, regulated expression of this specific inhibitor of granzyme B (13,18,33) in the liver accounts, at least in part, for the previously observed resistance of virally infected hepatocytes to perforin- and granzyme-dependent effector mechanisms (7) and, in turn, the greater importance of Fas and related death receptor-dependent cytotoxic effector mechanisms in immune-mediated injury and clearance of viral infections from the liver (8,9).

Indeed, inhibition of SPI-6 expression during hepatic viral infection leads to vigorous cytopathic immune responses resulting in severalfold higher serum alanine aminotransferase levels than observed in control mice and to the development of rapid onset, fatal acute liver failure in mice with deficient SPI-6 expression (22). The present findings indicate that unique feedback mechanisms allow the liver to rapidly up-regulate SPI-6 expression after exposure to granzyme B and perforin. This counterregulatory mechanism is likely, at least in part, responsible for the observation that vigorous cytopathic immune responses to hepatic viral infection only rarely lead to acute liver failure (36).

Acknowledgments

We acknowledge Christine Pham for providing DPP1-deficient mice, Timothy Ley for providing granzyme B mice, and John Schatzle, Michael Bennett, and Nitin Karandikar for their advice and constructive critique.

References

1. John B, Crispe IN. Passive and active mechanisms trap activated $CD8^+$ T cells in the liver. J. Immunol 2004;172:5222–5229. [PubMed: 15100260]
2. Wuensch SA, Pierce RH, Crispe IN. Local intrahepatic $CD8^+$ T cell activation by a non-self-antigen results in full functional differentiation. J. Immunol 2006;177:1689–1697. [PubMed: 16849478]
3. Khakoo SI, Thio CL, Martin MP, Brooks CR, Gao X, Astemborski J, Cheng J, Goedert JJ, Vlahov D, Hilgartner M, et al. HLA and NK cell inhibitory receptor genes in resolving hepatitis C virus infection. Science 2004;305:872–874. [PubMed: 15297676]
4. Shresta S, Heusel JW, Macivor DM, Wesselschmidt RL, Russell JH, Ley TJ. Granzyme B plays a critical role in cytotoxic lymphocyte-induced apoptosis. Immunol. Rev 1995;146:211–221. [PubMed: 7493755]
5. Thimme R, Wieland S, Steiger C, Ghrayeb J, Reimann KA, Purcell RH, Chisari FV. $CD8^+$ T cells mediate viral clearance and disease pathogenesis during acute hepatitis B virus infection. J. Virol 2003;77:68–76. [PubMed: 12477811]
6. Liu ZX, Govindarajan S, Kaplowitz N. Innate immune system plays a critical role in determining the progression and severity of acetaminophen hepatotoxicity. Gastroenterology 2004;127:1760–1774. [PubMed: 15578514]
7. Kafrouni MI, Brown GR, Thiele DL. Virally infected hepatocytes are resistant to perforin-dependent CTL effector mechanisms. J. Immunol 2001;167:1566–1574. [PubMed: 11466378]
8. Abougergi MS, Gidner SJ, Spady DK, Miller BC, Thiele DL. Fas and TNFR1, but not cytolytic granule-dependent mechanisms, mediate clearance of murine liver adenoviral infection. Hepatology 2005;41:97–105. [PubMed: 15619234]
9. Kafrouni MI, Brown GR, Thiele DL. The role of TNF-TNFR2 interactions in generation of CTL responses and clearance of hepatic adenovirus infection. J. Leukocyte Biol 2003;74:564–571. [PubMed: 12960267]
10. Pham CT, Ley TJ. Dipeptidyl peptidase I is required for the processing and activation of granzymes A and B in vivo. Proc. Natl. Acad. Sci. USA 1999;96:8627–8632. [PubMed: 10411926]
11. Liu CC, Detmers PA, Jiang SB, Young JD. Identification and characterization of a membrane-bound cytotoxin of murine cytolytic lymphocytes that is related to tumor necrosis factor/cachectin. Proc. Natl. Acad. Sci. USA 1989;86:3286–3290. [PubMed: 2654942]
12. Phillips T, Opferman JT, Shah R, Liu N, Froelich CJ, Ashton-Rickardt PG. A role for the granzyme B inhibitor serine protease inhibitor 6 in $CD8^+$ memory cell homeostasis. J. Immunol 2004;173:3801–3809. [PubMed: 15356127]
13. Sun J, Bird CH, Sutton V, McDonald L, Coughlin PB, De Jong TA, Trapani JA, Bird PI. A cytosolic granzyme B inhibitor related to the viral apoptotic regulator cytokine response modifier A is present in cytotoxic lymphocytes. J. Biol. Chem 1996;271:27802–27809. [PubMed: 8910377]
14. Bladergroen BA, Strik MC, Bovenschen N, van Berkum O, Scheffer GL, Meijer CJ, Hack CE, Kummer JA. The granzyme B inhibitor, protease inhibitor 9, is mainly expressed by dendritic cells and at immune-privileged sites. J. Immunol 2001;166:3218–3225. [PubMed: 11207275]

15. Buzza MS, Hirst CE, Bird CH, Hosking P, McKendrick J, Bird PI. The granzyme B inhibitor, PI-9, is present in endothelial and mesothelial cells, suggesting that it protects bystander cells during immune responses. Cell. Immunol 2001;210:21–29. [PubMed: 11485349]

16. Jiang X, Orr BA, Kranz DM, Shapiro DJ. Estrogen induction of the granzyme B inhibitor, proteinase inhibitor 9, protects cells against apoptosis mediated by cytotoxic T lymphocytes and natural killer cells. Endocrinology 2006;147:1419–1426. [PubMed: 16306080]

17. Medema JP, de Jong J, Peltenburg LT, Verdegaal EM, Gorter A, Bres SA, Franken KL, Hahne M, Albar JP, Melief CJ, Offringa R. Blockade of the granzyme B/perforin pathway through overexpression of the serine protease inhibitor PI-9/SPI-6 constitutes a mechanism for immune escape by tumors. Proc. Natl. Acad. Sci. USA 2001;98:11515–11520. [PubMed: 11562487]

18. Sun J, Ooms L, Bird CH, Sutton VR, Trapani JA, Bird PI. A new family of 10 murine ovalbumin serpins includes two homologs of proteinase inhibitor 8 and two homologs of the granzyme B inhibitor (proteinase inhibitor 9). J. Biol. Chem 1997;272:15434–15441. [PubMed: 9182575]

19. Tewari M, Beidler DR, Dixit VM. CrmA-inhibitable cleavage of the 70-kDa protein component of the U1 small nuclear ribonucleoprotein during Fas- and tumor necrosis factor-induced apoptosis. J. Biol. Chem 1995;270:18738–18741. [PubMed: 7543896]

20. Abdullah Z, Saric T, Kashkar H, Baschuk N, Yazdanpanah B, Fleischmann BK, Hescheler J, Kronke M, Utermohlen O. Serpin-6 expression protects embryonic stem cells from lysis by antigen-specific CTL. J. Immunol 2007;178:3390–3399. [PubMed: 17339433]

21. Barrie MB, Stout HW, Abougergi MS, Miller BC, Thiele DL. Antiviral cytokines induce hepatic expression of the granzyme B inhibitors, proteinase inhibitor 9 and serine proteinase inhibitor 6. J. Immunol 2004;172:6453–6459. [PubMed: 15128837]

22. Stout-Delgado HW, Getachew Y, Rogers TE, Miller BC, Thiele DL. The role of serpinb9/serine protease inhibitor 6 in preventing granzyme B dependent hepatotoxicity. Hepatology. 2007In press

23. Revell PA, Grossman WJ, Thomas DA, Cao X, Behl R, Ratner JA, Lu ZH, Ley TJ. Granzyme B and the downstream granzymes C and/or F are important for cytotoxic lymphocyte functions. J. Immunol 2005;174:2124–2131. [PubMed: 15699143]

24. Brown GR, Thiele DL, Silva M, Beutler B. Adenoviral vectors given intravenously to immunocompromised mice yield stable transduction of the colonic epithelium. Gastroenterology 1997;112:1586–1594. [PubMed: 9136837]

25. Salazar-Mather TP, Lewis CA, Biron CA. Type I interferons regulate inflammatory cell trafficking and macrophage inflammatory protein 1α delivery to the liver. J. Clin. Invest 2002;110:321–330. [PubMed: 12163451]

26. Yang H, Dithmar S, Grossniklaus HE. Interferon α 2b decreases hepatic micrometastasis in a murine model of ocular melanoma by activation of intrinsic hepatic natural killer cells. Invest. Ophthalmol. Vis. Sci 2004;45:2056–2064. [PubMed: 15223777]

27. Goossens PL, Jouin H, Marchal G, Milon G. Isolation and flow cytometric analysis of the free lymphomyeloid cells present in murine liver. J. Immunol. Methods 1990;132:137–144. [PubMed: 2202764]

28. Watanabe H, Ohtsuka K, Kimura M, Ikarashi Y, Ohmori K, Kusumi A, Ohteki T, Seki S, Abo T. Details of an isolation method for hepatic lymphocytes in mice. J. Immunol. Methods 1992;146:145–154. [PubMed: 1531671]

29. McGuire MJ, Lipsky PE, Thiele DL. Generation of active myeloid and lymphoid granule serine proteases requires processing by the thiol protease dipeptidyl peptidase I. J. Biol. Chem 1993;268:2458–2467. [PubMed: 8428921]

30. Brown GR, McGuire MJ, Thiele DL. Dipeptidyl peptidase I is enriched in granules of in vitro- and in vivo-activated cytotoxic T lymphocytes. J. Immunol 1993;150:4733–4752. [PubMed: 8496587]

31. Brown GR, Meek K, Nishioka Y, Thiele DL. CD27-CD27 ligand/ CD70 interactions enhance alloantigen-induced proliferation and cytolytic activity in $CD8^+$ T lymphocytes. J. Immunol 1995;154:3686–3695. [PubMed: 7706711]

32. Strik MC, Bladergroen BA, Wouters D, Kisiel W, Hooijberg JH, Verlaan AR, Hordijk PL, Schneider P, Hack CE, Kummer JA. Distribution of the human intracellular serpin protease inhibitor 8 in human tissues. J. Histochem. Cytochem 2002;50:1443–1454. [PubMed: 12417609]

33. Kaiserman D, Knaggs S, Scarff KL, Gillard A, Mirza G, Cadman M, McKeone R, Denny P, Cooley J, Benarafa C, et al. Comparison of human chromosome 6p25 with mouse chromosome 13 reveals a greatly expanded ov-serpin gene repertoire in the mouse. Genomics 2002;79:349–362. [PubMed: 11863365]

34. Sun J, Whisstock JC, Harriott P, Walker B, Novak A, Thompson PE, Smith AI, Bird PI. Importance of the P4′ residue in human granzyme B inhibitors and substrates revealed by scanning mutagenesis of the proteinase inhibitor 9 reactive center loop. J. Biol. Chem 2001;276:15177–15184. [PubMed: 11278311]

35. Wang X, Zelenski NG, Yang J, Sakai J, Brown MS, Goldstein JL. Cleavage of sterol regulatory element binding proteins (SREBPs) by CPP32 during apoptosis. EMBO J 1996;15:1012–1020. [PubMed: 8605870]

36. Rehermann B, Nascimbeni M. Immunology of hepatitis B virus and hepatitis C virus infection. Nat. Rev. Immunol 2005;5:215–229. [PubMed: 15738952]

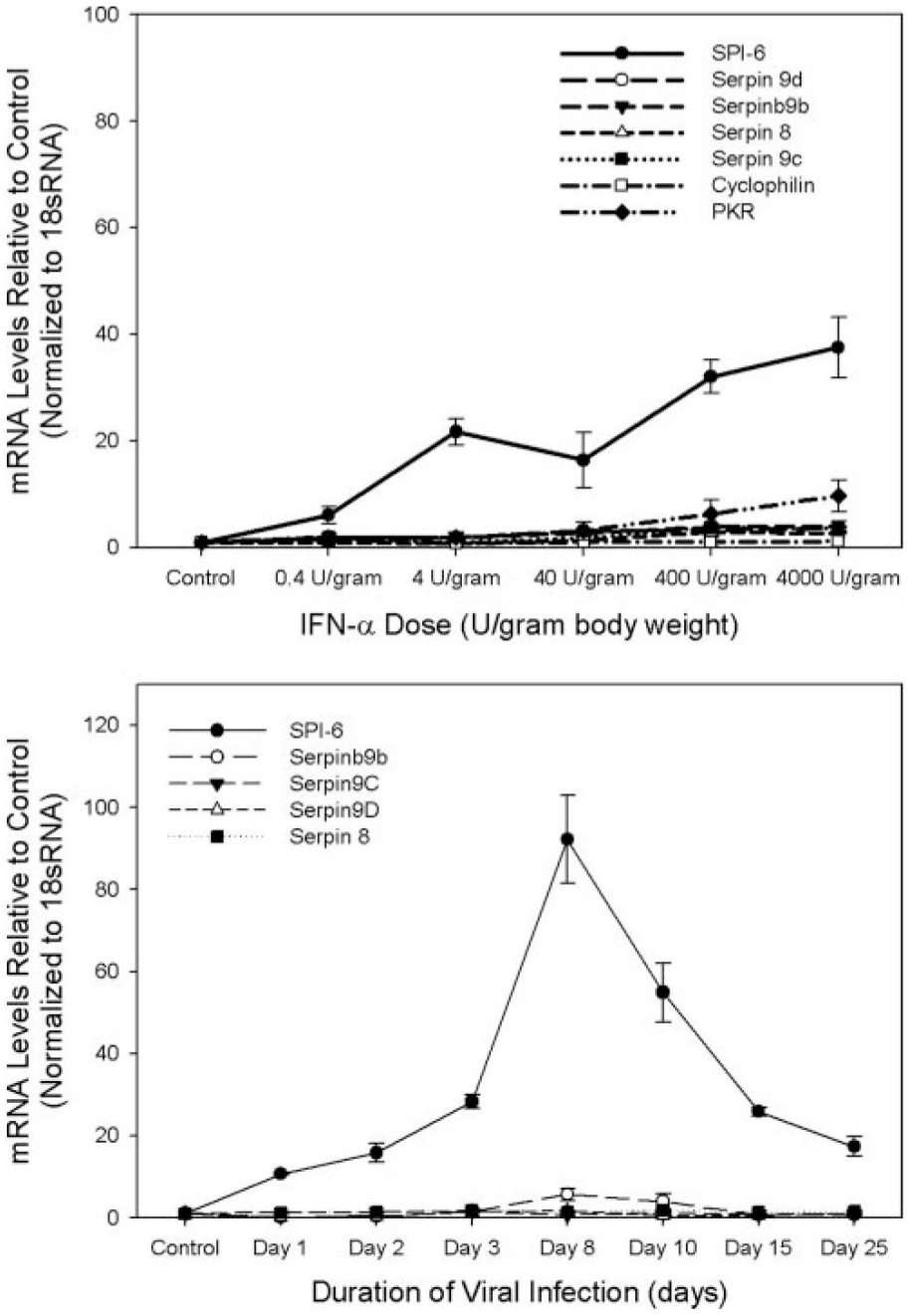

FIGURE 1.

Evaluation of *serpinB9* homolog expression in vivo after treatment with antiviral cytokines and during the AdCMV-*LacZ* infection. *Top panel*, RNA was isolated from the livers of B6 mice 24 h after treatment with the indicated doses of IFN-*α*. *SerpinB9* homolog, cyclophilin, and PKR mRNA expression was analyzed using real-time PCR and results were normalized to 18S RNA. The values presented are the mean ± SE of determinations from three mice in each experimental group. *Bottom panel*, RNA was isolated from the livers of B6 mice at specific time points during the course of AdCMV-*LacZ* infection. *SerpinB9* homolog mRNA expression was analyzed using real-time PCR and results were normalized to 18S RNA. The values presented represent the mean ± SE of determinations of mRNA expression relative to

control from three to nine mice per experimental group. The data are representative of three experiments with similar results.

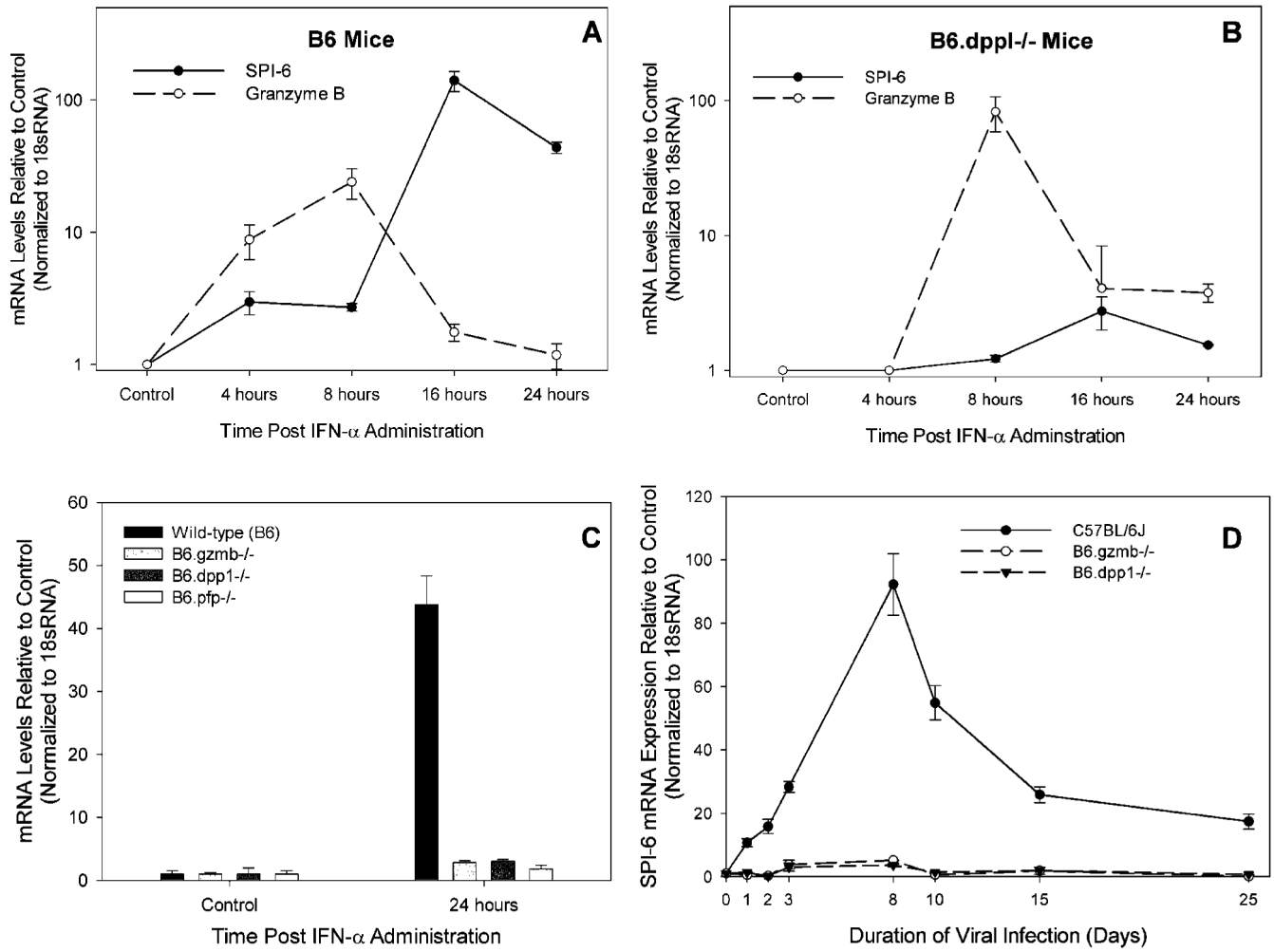

FIGURE 2.

Analysis of SPI-6 mRNA expression in wild-type and granzyme B-deficient transgenic mice. RNA was isolated from the livers of experimental mice at specific time points after IFN-*α* administration and granzyme B and SPI-6 mRNA expression in B6 (*A*) or B6.*dppi*$^{-/-}$ mice (*B*) was assessed by real-time PCR and normalized to endogenous 18S RNA. *C*, SPI-6 mRNA expression in liver of B6, B6.*dpp1*$^{-/-}$, B6.*gzmb*$^{-/-}$, and/or B6.*pfp*$^{-/-}$ mice was analyzed at specific time points after IFN-*α* administration or during the viral infection in the liver of wild-type and granzyme B-transgenic mice in which RNA was isolated from the livers of experimental mice at specific time points during AdCMV-*LacZ* infection and SPI-6 mRNA expression in liver of B6, B6.*dpp1*$^{-/-}$, or B6.*gzmb*$^{-/-}$ mice (n = 6–9 mice/time point). Each bar represents the mean ± SD of triplicate determinations of mRNA expression relative to control and normalized to 18S RNA.

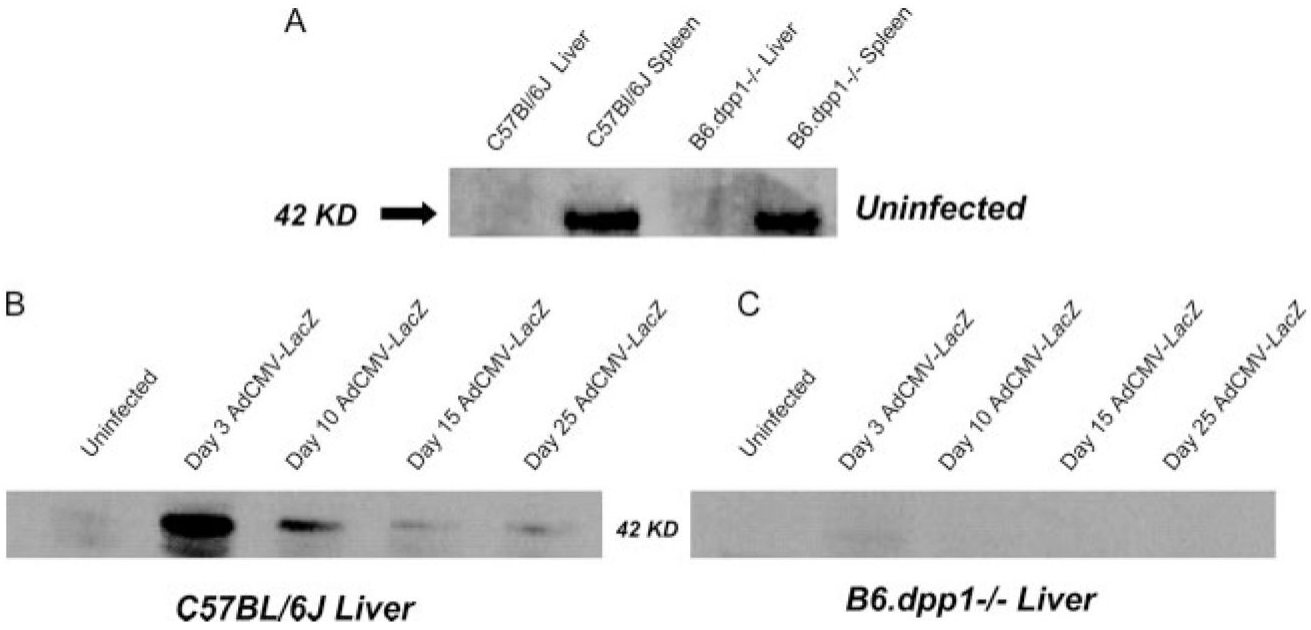

FIGURE 3.

A–C, SPI-6 protein levels in liver of C57BL/6J and B6.*dpp1*$^{-/-}$ mice during AdCMV-*LacZ* infection. Protein lysates from uninfected, AdCMV-*LacZ*-infected C57BL/6J or B6.*dpp1*$^{-/-}$ mice were prepared as detailed in *Materials and Methods*. Protein levels were assayed and 20 μg of protein was loaded per lane before SDS-PAGE separation of proteins and immunoblotting with SPI-6-specific Ab. Data represent the results of one of several experiments with similar results.

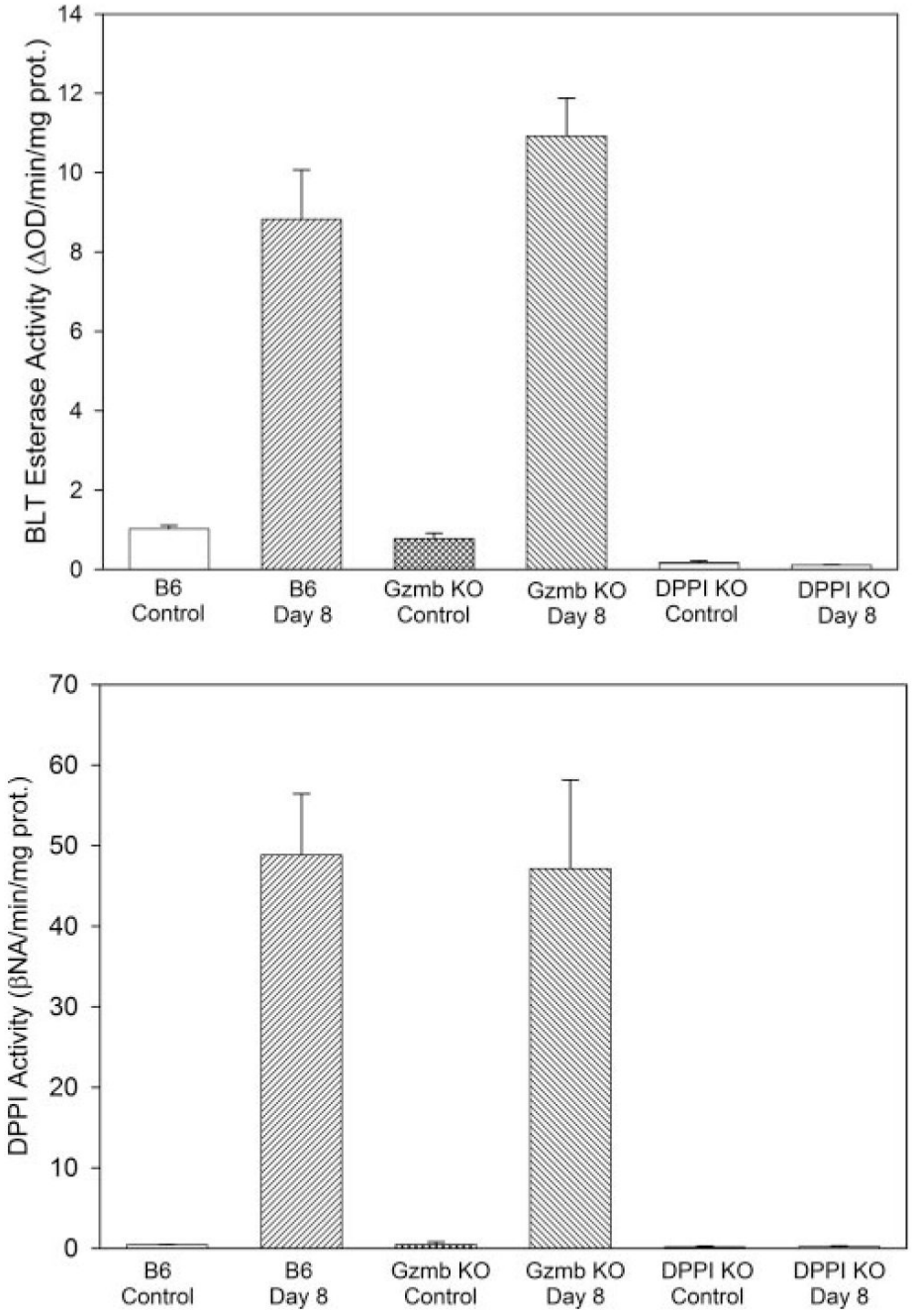

FIGURE 4.

Evaluation of lymphocyte activation in B6, B6.*dpp1*$^{-/-}$, and B6.*gzmb*$^{-/-}$ mice during AdCMV-*LacZ* infection. BLT esterase (*top panel*) and DPPI (*bottom panel*) assays as described in *Materials and Methods*, were performed on intrahepatic lymphocytes isolated from control and day 8 AdCMV-*LacZ*-infected mice.

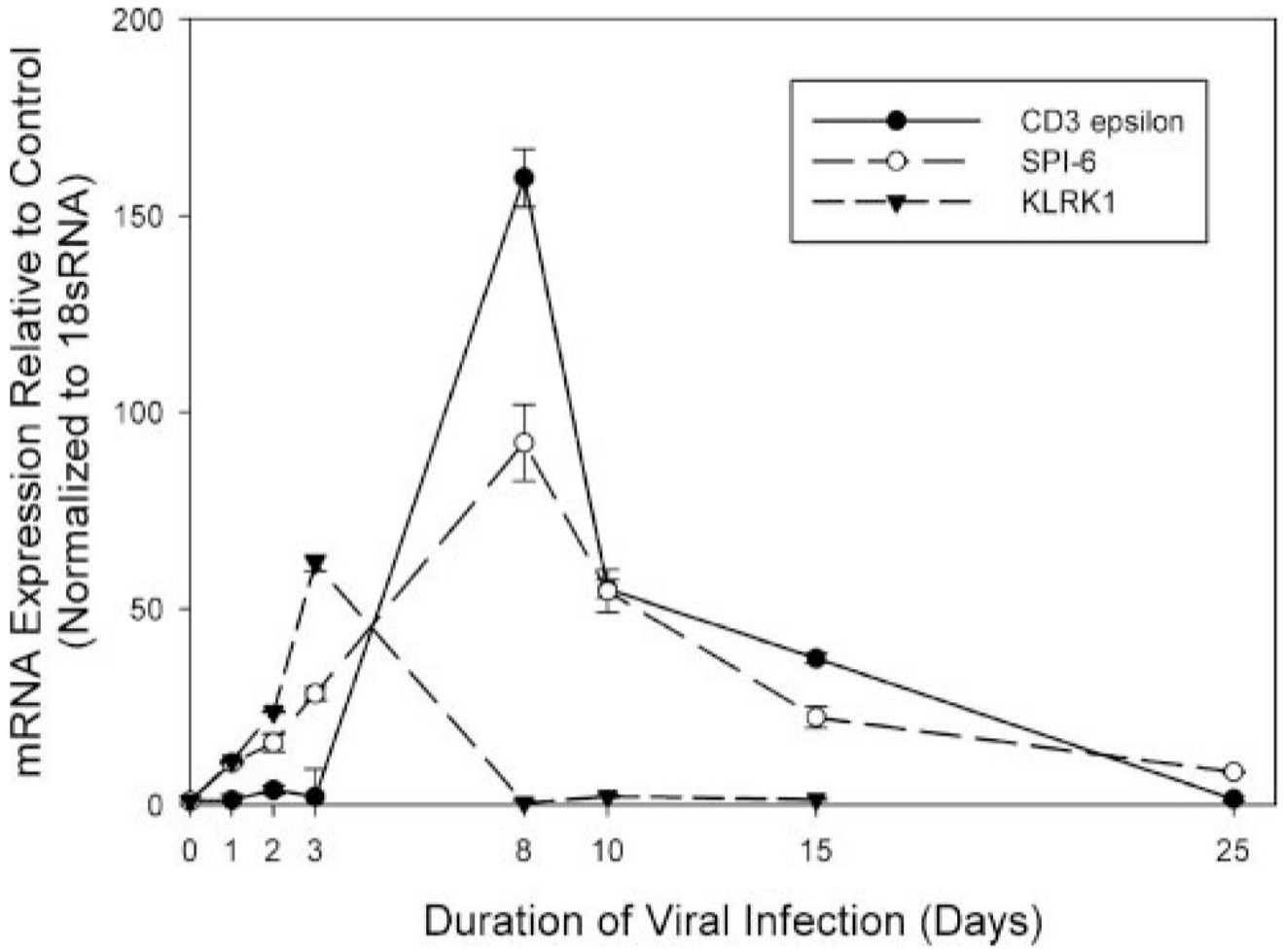

FIGURE 5.

KLRK1 and CD3*ε* mRNA levels during the course of AdCMV-*LacZ* infection correspond with SPI-6 mRNA expression levels. RNA was isolated from livers of control and virally infected mice at specific time points during viral infection. Relative KLRK1 and CD3*ε* mRNA levels were quantified using real-time PCR. Each bar represents the mean ± SD of triplicate determinations of mRNA expression relative to control and normalized to 18S RNA. Data are representative of several experiments with similar results.

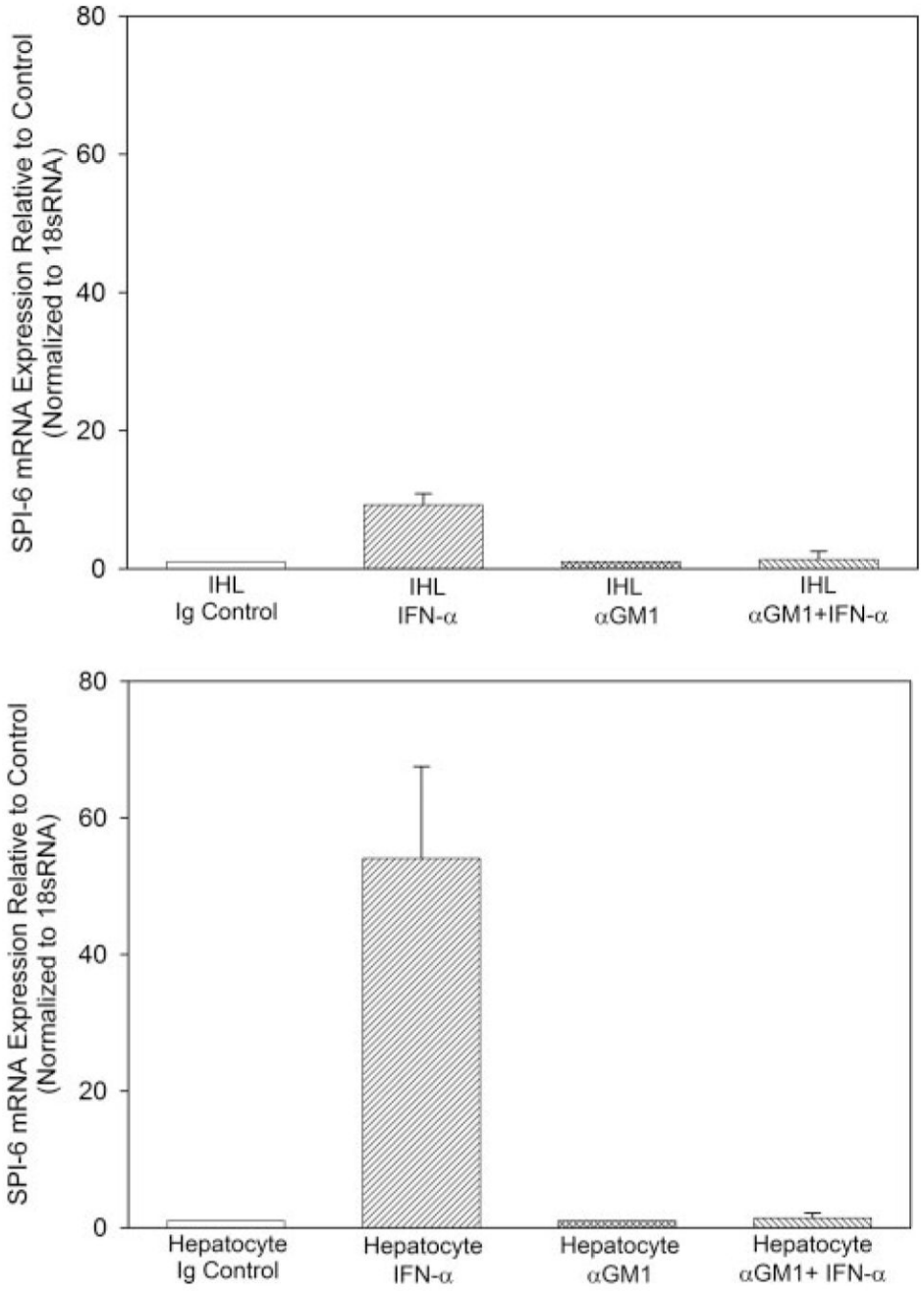

FIGURE 6.

SPI-6 mRNA expression in intrahepatic lymphocytes and hepatocytes isolated from C57BL/6J mice. Intrahepatic lymphocytes (*top panel*) and hepatocytes (*bottom panel*) were isolated from wild-type or anti-asialo GM1-treated mice as described in *Materials and Methods*. RNA was isolated and relative SPI-6 mRNA expression was analyzed using real-time PCR. Each bar represents the mean ± SD of triplicate determinations of mRNA expression relative to control samples and normalized to 18S RNA. Data are representative of three experiments with similar results.

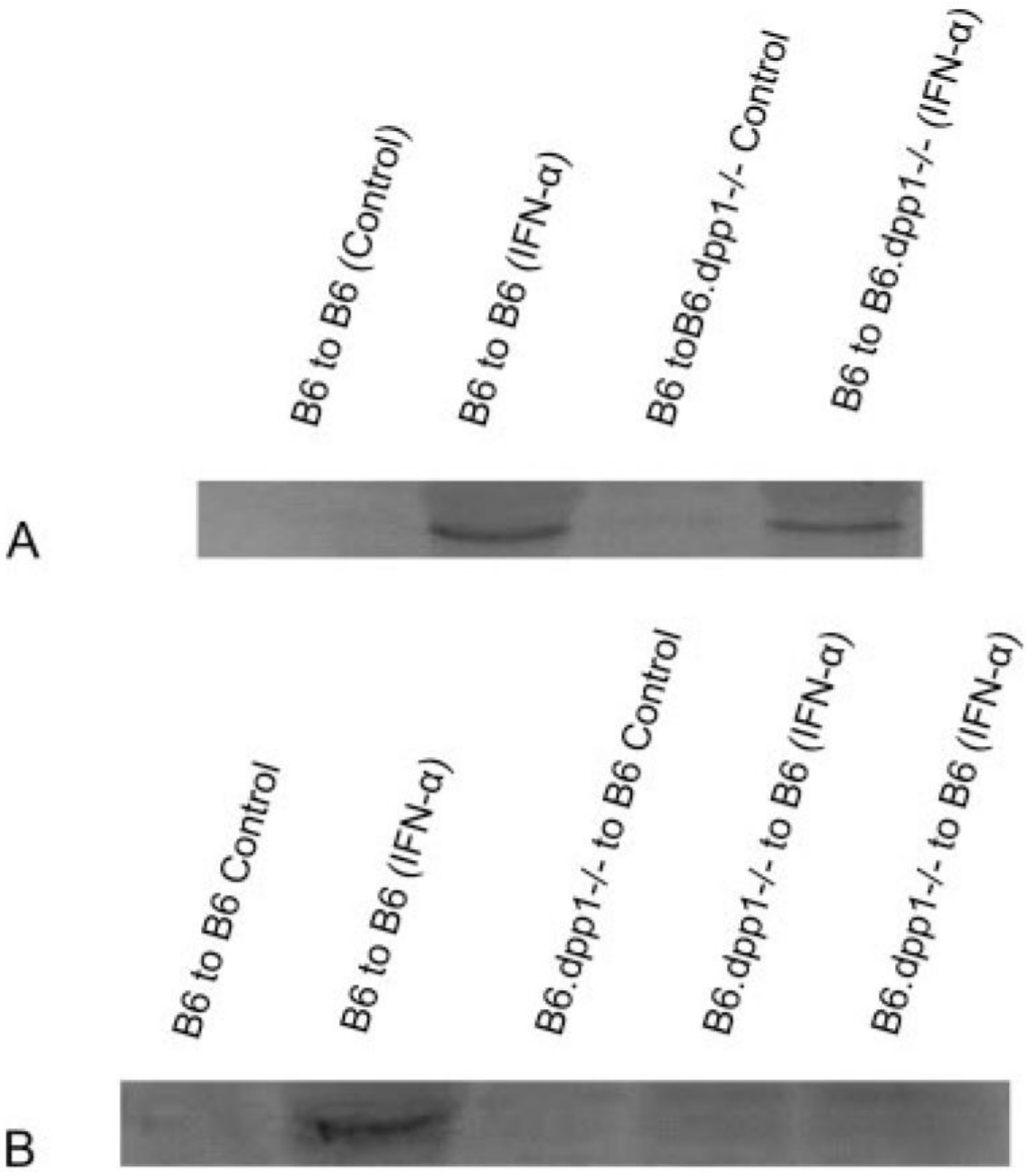

FIGURE 7.

A and *B*, SPI-6 protein levels in bone marrow transplant chimeric mice. Protein lysates from bone marrow transplant chimeric mice, B6 to B6.dpp1$^{-/-}$ and B6.dpp1$^{-/-}$ to B6 were prepared as detailed in *Materials and Methods*. Protein levels were assayed and 20 μg of protein was loaded per lane before SDS-PAGE separation of proteins and immunoblotting with SPI-6-specific Ab. Data represent the results of one of several experiments with similar results.

Table I

Real-time RT-PCR primers

Gene	Forward Primer	Reverse Primer
Cyclophilin	5′—gcccgtagtgcttcagctt—3′	5′—ggagatggcacaggaggaa—3′
18S RNA	5′—gcctcagttccgaaaacca—3′	5′—ccgcagctaggaataatgga—3′
Serpinb9	5′—tatctcaggcacttggtttgaataaa—3′	5′—tttctgtctggcttgttcagctt—3′
Serpinb9b	5′—caagcccacatccctttgaa—3′	5′—tgttggcagatgactcagttaatttc—3′
Serpinb9c	5′—ttgggaggaattcacaagtgttc—3	5′—gaagccaaccagaaagtacacctt—3′
Serpinb9e	5′—acagcatttgggaatcttgg—3′	5′—gcaacagcctctgttccttc—3′
Serpinb9f	5′—acaacccttcaaaaatgtgtgttat—3′	5′—gtctcccttagcacccaagaga—3′
Serpinb9g	5′—gaccagtgcagatgatgttgg—3′	5′—cactagcacttgtgcctgga—3
CD3ϵ	5′—ggacagtggctactacgtctgcta—3′	5′—tgatgattatggctactgctgtca—3′
KLRK1	5′—gctatagccttggcaattcg—3′	5′—gccacagtagccctctcttg—3′